Research Article

Micro-computed tomography utility for estimation of intraparenchymal spinal cord cystic lesions in small animals

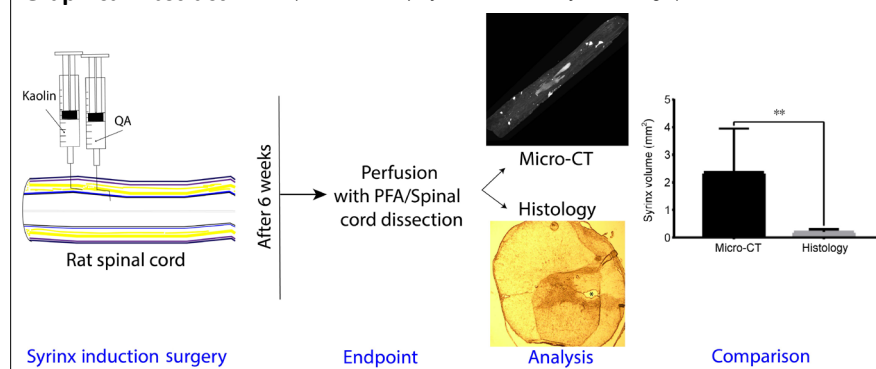Mahmoud Farrag[1], Dipak D. Pukale[2], Nic D. Leipzig[3, *]

Graphical Abstract *A comparative study of two methods of assessing spinal cord lesion size*

Abstract

Precise assessment of spinal cord cystic lesions is crucial to formulate effective therapeutic strategies, yet histological assessment of the lesion remains the primary method despite numerous studies showing inconsistent results regarding estimation of lesion size via histology. On the other hand, despite numerous advances in micro-computed tomography (micro-CT) imaging and analysis that have allowed precise measurements of lesion size, there is not enough published data on its application to estimate intraspinal lesion size in laboratory animal models. This work attempts to show that micro-CT can be valuable for spinal cord injury research by demonstrating accurate estimation of syrinx size and compares between micro-CT and traditional histological analysis. We used a post-traumatic syringomyelia rat model to compare micro-CT analysis to conventional histological analysis. The study showed that micro-CT can detect lesions within the spinal cord very similar to histology. Importantly, micro-CT appears to provide more accurate estimates of the lesions with more measures (e.g., surface area), can detect compounds within the cord, and can be done with the tissue of interest (spinal cord) intact. In summary, the experimental work presented here provides one of the first investigations of the use of micro-CT for estimating the size of intraparenchymal cysts and detecting materials within the spinal cord. All animal procedures were approved by the University of Akron Institutional Animal Care and Use Committee (IACUC) (protocol # LRE 16-05-09 approved on May 14, 2016).
Key Words: cyst size; histology; intraparenchymal cysts; lesion size estimate; micro-CT; post-traumatic syringomyelia; spinal cord imaging; spinal cord injury; spinal cystic lesion; syrinx

Chinese Library Classification No. R445; R364; R741

Introduction

Formation of cystic lesions inside the spinal cord parenchyma, either primarily or secondary to other neurological conditions, is a well-known neurological problem and it is called syringomyelia (Klekamp, 2002; Al-Shatoury and Galhom, 2017). These cystic lesions expand and exert pressure on the adjacent neural tissues, which causes further damage to the neural tissues. Intraparenchymal cyst formation deteriorates the quality of life of about 30% of spinal cord injury (SCI) patients and 8.4 individuals per 100,000 in USA (Disorders, 2016). Moreover, these intraparenchymal cysts are found in many experimental models of SCI (Fraidakis et al., 1998).

Clinically, cysts are diagnosed and followed up using imaging techniques, such as magnetic resonance imaging (MRI), which is the gold standard imaging modality. In research settings, the study of syrinxes requires an accurate calculation of syrinx size *in situ*. Thus, researchers often employ histological techniques that enable them to estimate lesion sizes based on the section thickness, number of sections, and distance between consecutive sections. Multiple attempts have been made previously to increase the accuracy of lesion size estimations from histological sections (Park et al., 2013).

Imaging techniques are not widely used in animal studies that focus on SCI or post-traumatic syringomyelia (PTSM)

[1]Integrated Bioscience Program, The University of Akron, Akron, OH, USA; [2]Department of Chemical, Biomolecular, and Corrosion Engineering, The University of Akron, Akron, OH, USA; [3]Department of Chemical, Biomolecular, and Corrosion Engineering, Integrated Bioscience Program, The University of Akron, Akron, OH, USA
*Correspondence to: Nic D. Leipzig, PhD, nl21@uakron.edu.
https://orcid.org/0000-0002-6356-7691 (Nic D. Leipzig)

Research Article

based on a current review of the number of publications published on this topic. Perhaps, the variety of applications cannot all be covered by one imaging technique, and it would be expensive to use multiple imaging modalities. Recently, there is renewed interest in the use of imaging techniques in animal studies (Schambach et al., 2010; Webb et al., 2016) to improve upon analysis techniques. Regarding the study of syringomyelia, even though histology is the mainstream technique to study cysts, it is challenging, considering the size of the animal's spinal cord and the size of the lesion inside it. Moreover, histological analysis is technically demanding, time-consuming, and can lead to significant tissue distortion (Dauguet et al., 2007; Ohnishi et al., 2016). Thus, another validating test for syringomyelia research would be helpful when histology is employed for lesion size calculations. Many studies that investigate imaging techniques as an alternative for, or supportive to, histological analysis focus on the use of MRI, particularly in live animals (Fraidakis et al., 1998; Dauguet et al., 2007; Engelhorn et al., 2009; Saito et al., 2012; Dalkilic et al., 2018), as done by Schwartz et al. (1999) and Najafi et al. (2016). Animal MRI, however, is expensive, not broadly available, and requires specific technical skills for its interpretation (de Crespigny et al., 2008).

Recent advances in the field of X-ray tomography have encouraged researchers to investigate the utility of micro-CT in research applications (Hsieh et al., 2013). As such, studies have utilized laboratory-based micro-computer tomography (micro-CT) systems to visualize various tissues with excellent resolution (Saito et al., 2012; Gignac and Kley, 2018). However, most studies have focused on tissues with high-density such as osseous structures (Campbell and Sophocleous, 2014), dental tissues (Özkan et al., 2015; Boca et al., 2017), and contrast-injected vascular networks (Schambach et al., 2010; Campbell and Sophocleous, 2014), with little focus on soft tissues like the central nervous system. The performance of micro-CT in neural tissue evaluation is restricted due to limited contrast (Zehbe et al., 2010). Many attempts have been made to improve the contrast between neural tissues such as the use of contrast agents to visualize the brain (de Crespigny et al., 2008; Gignac and Kley, 2018) and peripheral nerves (Pixley et al., 2016; Bikis et al., 2018), and the use of paraffin-embedded cerebral tissues (Khimchenko et al., 2016). These improvements made micro-CT a more convenient research tool in neural research (de Crespigny et al., 2008). While micro-CT has been evaluated for use with different tissues in general and neural tissues in particular, no single study, to the best of our knowledge, exists assessing the utility of conventional micro-CT in evaluating cystic lesions inside the spinal cord.

Therefore, the main purpose of this work was to investigate conventional micro-CT, a broadly available imaging technique, as a reliable tool to assess spinal cord cystic lesions at the endpoint in comparison to traditional histological analysis. To the best of our knowledge, this is the first study to explore the use of conventional micro-CT in quantifying syrinx size in PTSM in an animal model and it aims to contribute to this growing area of research by comparing syrinx measurements using micro-CT analysis with histological analysis.

Materials and Methods

Ethics statement
All procedures (protocol # LRE 16-05-09) that involved animals were approved by the University of Akron Institutional Animal Care and Use Committee (IACUC) on May 14, 2016. All surgical procedures were performed under aseptic conditions (aseptic preparation of surgical field, shaving of the rat fur, scrubbing the skin with povidone-iodine solution and alcohol, draping, wearing a cap, sterile gloves, mask, and appropriate surgical attire, sterile instruments).

Syrinx induction surgeries
Studies were conducted on eight 12-week-old male Wistar rats with body weight between 350–450 g (Envigo, Haslett, MI, USA) following syrinx induction procedure published previously (Mohrman et al., 2017). The rats are acclimatized at the University of Akron animal facility for a week before performing any surgeries. The rat room had a controlled 12/12-hour light/dark cycle (lights on at 7:00 a.m.), temperature (22 ± 2°C), and relative humidity (30–70%). They were kept two per cage. For the PTSM injury model, rats were first anesthetized using isoflurane (Penn Veterinary Supply, Inc. Lancaster, PA, USA) inhalation. To induce syrinx formation, a C7-T1 laminectomy was performed and the spinal cord was exposed. Two injections were done using a 10 μL syringe with a 27G needle with a precision sleeve. The first injection was 2 μL of 24 mg/mL quisqualic acid (Enzo Life Sciences, Farmingdale, NY, USA) into the spinal cord parenchyma and the second injection was 5 μL of 250 mg/mL kaolin (Avantor, Center Valley, PA, USA) into the subarachnoid space. All liquids (including solvent, compounds) that were used for injection in animals were sterilized either by 15-minute liquid cycle in the autoclave or through filtration. NNC 05-2090 (TOCRIS, Minneapolis, MN, USA), gamma-aminobutyric acid uptake inhibitor that displays moderate selectivity for the BGT-1 channel, is the drug that was selected to be tested to study its retention inside the spinal cord parenchyma. The injection of 20 μL of NNC 05-2090, as well as other tested materials such as dimethyl sulfoxide (DMSO), was performed in post-mortem spinal cords of naïve rats that had not undergone any live surgeries.

Animal sacrifice and tissue harvest
For the purpose of tissue collection for analysis, animals were sacrificed according to the policies of the University of Akron. Six weeks after the syrinx induction surgery, to ensure the formation of syrinx in all rats according to published data from Dr. Stoodley lab (Brodbelt et al., 2003) and as confirmed by our previous studies (Mohrman et al., 2017), rats were administered an overdose of ketamine/acepromazine/xylazine (supplied by the University of Akron animal facility staff) intramuscularly based upon a dosage range of 150 mg/kg ketamine, 30 mg/kg xylazine, and 4.5 mg/kg acepromazine; once the animals were sufficiently anesthetized and the heart had slowed, the ribs were opened, and the heart was exposed. An 18G needle was inserted through the left ventricle into the ascending aorta. The needle was kept visible inside the ascending aorta and was clamped in the ascending aorta to prevent slipping. The right atrium was incised to allow fluid to flow out. A peristaltic pump was used at 15 mL/min to perfuse the animals with heparin (Sigma-Aldrich, St. Louis, MO, USA) first. Then animals were transcardially perfused with 3.7% fresh paraformaldehyde. Finally, an extensive laminectomy was done to expose the spinal cord, and then the spinal cord was removed gently.

Spinal cord micro-CT imaging and analysis
After perfusing rats with an intraspinal cyst, spinal cords were immediately harvested and washed in phosphate buffered saline (PBS). The cords were post-fixed overnight and maintained in PBS until scanned. Fixed spinal cord segments were scanned using a micro-CT scanner (SkyScan 1172, Bruker, Kontich, Belgium) before sectioning. Scanning was done for 360O with an image pixel size of 12.05 μm, no filter and medium camera at 70 kV, 141 mA, and 40 V. Reconstruction of the images was done using NRecon software (Bruker) with smoothing and ring artifact correction. The reconstructed images underwent further processing using CT Analyzer (Bruker) and MIMICS software (Materialise, Leuven, Belgium), and manual segmentation was done to isolate the cystic lesions from spinal cord parenchyma. Three-dimensional (3D) reconstruction and measurement of the lesion were done automatically through the software.

Histology and immunohistochemistry

Eight spinal cord samples were washed in PBS after harvesting, post-fixed overnight, washed in PBS, then equilibrated in 30% sucrose until the sample sunk to the bottom of the tube. When samples were equilibrated and cryoprotected, the samples were cut into 3-cm length segments, embedded in optimal cutting temperature (OCT) compound. The OCT mold including the spinal cord samples were kept on dry ice until samples froze, then stored in -80oC until sectioning. The spinal cord segments were sectioned using a cryostat (Leica CM 1850, Wetzlar, Germany) on glass slides to the desired thickness of 25 μm and every fifth section was collected.

For the purpose of sample labeling, the monoclonal mouse anti-Iba1 antibody (1:50, Cat # sc-32725, Santa Cruz Biotechnology, Dallas, TX, USA) was used to identify microglia activation related to syrinx formation by incubating the tissue with the primary antibody overnight at 4°C after tissues were blocked with 10% goat serum in 1× PBS at room temperature (RT) for 30 minutes. Prior to incubating sections with goat anti-mouse Alexa Fluor® 488 secondary antibodies (1:400, Cat# ab150113, Abcam, Cambridge, UK), sections were washed three times with PBS, with each wash lasted at least 15 minutes. The incubation lasted for at least 1 hour at RT and was followed by an additional three 15-minute PBS washes. The final stage was staining cell nuclei with 1 μg/mL Hoechst 33342 in PBS (henceforth referred to as DAPI when imaging since the same emission/excitation settings are used) for 7 minutes, followed by mounting using ProLong™ Gold Antifade (ThermoFisher, Waltham, MA, USA). Controls where the primary antibody was omitted, were performed throughout to determine if any non-specific staining existed to confirm staining. Slides were imaged using an Olympus IX81 fluorescent microscope (Olympus, Tokyo, Japan) or an Olympus FV1000 confocal microscope (Olympus), then processed using MetaMorph software version 7.10 (Molecular Devices, Sunnyvale, CA, USA).

Spinal cord sections used for syrinx size estimation were imaged with an Olympus CKX41 (Olympus) inverted light microscope without staining. The images were then processed using ImageJ software. Finally, the processed images were segmented manually to isolate lesions that could be a cyst, and then lesions were measured in each fifth section. To determine the total volume for a lesion, first the crosectional surface area of each lesion were calculated in sections that encompassed the syrinx then averaged. The total volume was then calculated by multiplying the average surface area by the total distance between consecutive sections with a lesion.

Statistical analysis

Statistical analyses were performed using JMP Pro 13 (SAS Institute, Cary, NC, USA) and Prism 8 (GraphPad Software, Inc., San Diego, CA, USA) software. Data were analyzed using paired t-tests with $\alpha = 0.05$ to detect significant differences between the two methods of analyzing syrinx size. Data were presented as mean ± standard deviation (SD).

Results

Descriptive evaluation

Histology is a well-established technique to investigate anatomical structures and abnormalities. This study set out with the objective to evaluate the utility of micro-CT in the evaluation/quantification of cystic lesions in the spinal cord and to determine the ability of micro-CT to be utilized as an adjunct method for spinal cord cystic lesions size estimation. Preliminary assessment of the histological sections indicated the development of pathological changes in the spinal cord as noted in the presence of cystic and hematoma like abnormalities, which corresponded to similar lesions in the corresponding micro-CT slices (**Figure 1**).

Figure 1 compares representative images of different spinal cords. Each section was evaluated with a brightfield microscope and matched with a correlative level evaluated using micro-CT. Each histological section was a 25-μm segment of the spinal cord, while micro-CT images represented very thin (< 10 μm) slices of the spinal cord; therefore, the correlated histological and micro-CT images are approximate. Both histological and tomographical evaluation was able to detect cystic lesions (**Figure 1**) and hematoma-like lesions (**Figure 1**) in different regions of the spinal cord. The site and shape of lesions in the micro-CT images closely matched the corresponding histological sections.

Foreign material injection detection ability of micro-CT

The injury model that was established in our lab for PTSM (Mohrman et al., 2017) utilizes several chemicals that are injected into the spinal cord directly or its subarachnoid space, which may eventually end inside spinal cord parenchyma. Furthermore, previous work has established that kaolin injected into these sites leads to parenchymal migration and accumulation (Cho et al., 1994; Brodbelt et al., 2003; Hemley et al., 2009; Mohrman et al., 2017). Moreover, this model can be used to evaluate the effect of specific delivered compounds on syrinx size (Mohrman et al., 2018). Therefore, the ability of micro-CT to detect treatments inside the spinal cord parenchyma would be of high value. Using post-mortem segments, several compounds were injected directly inside a spinal cord segment, and micro-CT scanning was performed to test the technique's ability to detect these materials (**Figure 2**). Micro-CT images of segments injected with DMSO (**Figure 2A**), NNC 05-2090 (**Figure 2B**), and quisqualic acid (**Figure 2C**) do not show any enhanced signals of radiodensity. Instead, they show a cystic cavity (denoted with asterisks) that might have resulted due to the wide caliber needle used to inject these materials in the spinal cord parenchyma. On the other hand, the segments injected with kaolin (**Figure 2D**, indicated with black arrows) and a chitosan-based biomaterial delivery system (Mohrman et al., 2018) (**Figure 2E**) show radio-opaque materials inside the spinal cord parenchyma.

Immunohistological confirmation of syrinxes

Since histological sections of delicate tissue, such as the spinal cord, tend to crack and break during sectioning, we wanted to confirm that cystic lesions observed in these sections represented syrinxes formed due to the injected excitotoxic quisqualic acid. Therefore, Iba1, a microglia marker, was used to identify the areas of central nervous system inflammatory cell accumulation in response to the primary injury. As shown in **Figure 3**, the results obtained from immunohistochemical staining provide evidence of cystic lesion formation. **Figure 3** shows a representative image of a cystic lesion (denoted with an asterisk) surrounded by Iba1 positive cells, while **Figure 3** presents other evidence of a cystic lesion (denoted with an asterisk) and aggregation of cells is nearby, which include many Iba1 positive cells, which is suggestive of microglial activation near the injury site.

Measurement of syrinxes using micro-CT and comparison to histology

For any treatment modality that is proposed for cystic lesions, cyst measurement will be an essential response to be assessed. As the goal of syringomyelia therapy should be to reduce the cyst size, and therefore an accurate measure of the cyst is very critical to evaluate the effect of proposed therapies. **Figure 4** shows a comparison between cyst measurements as evaluated by micro-CT and by histology methods in terms of syrinx area and syrinx volume. Both surface area ($P = 0.002$; **Figure 4**) and volume ($P = 0.006$; **Figure 4**) measurements revealed a significant difference between histology and micro-CT. Interestingly, micro-CT estimation was always higher than histological estimates.
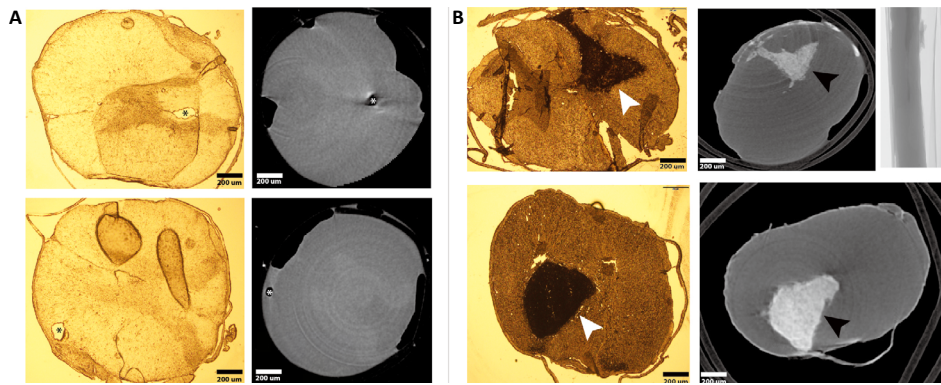
Figure 1 | Representative images from micro-CT and histological sections showing changes in the spinal cord after syrinx induction.
(A) Axial views showing syrinxes as hypodense areas in both histological sections and micro-CT images (marked with asterisks). (B) Images show large hyperdense areas (marked with arrowheads) within the spinal cord parenchyma in both histological sections and micro-CT images. These areas likely are a hematoma or accumulation of the injected kaolin material. micro-CT: Micro-computed tomography.
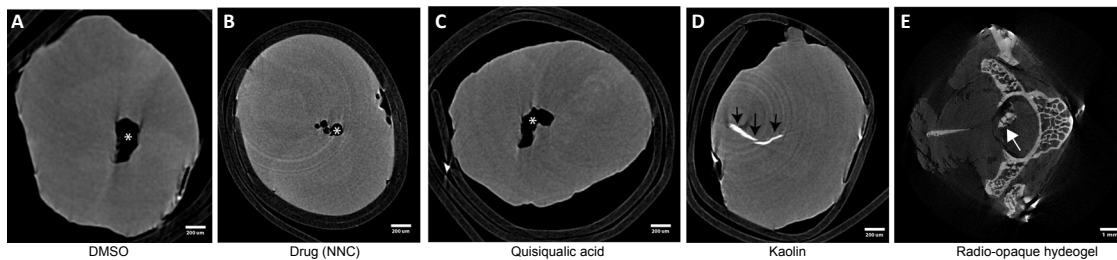
Figure 2 | The micro-CT capacity to detect intraspinal abnormalities such as post-mortem induced cystic lesions (A–C), intraspinal kaolin (D), and intraspinal injected hydrogel (E).
Black arrows point to the kaolin. Asterisks denote cysts, and white arrow denotes an intraparenchymal hydrogel. DMSO: Dimethyl sulfoxide; micro-CT: Micro-computed tomography; NNC: gamma-aminobutyric acid uptake inhibitor NNC 05-2090.
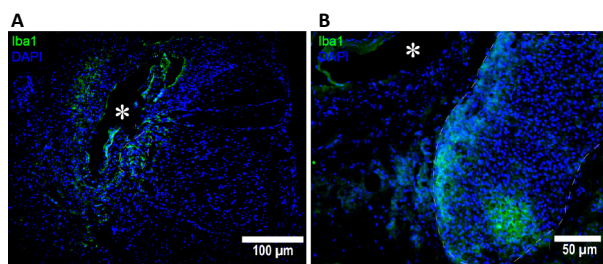

Figure 3 | Histological confirmation of premortem cyst formation using Iba1, microglia antibody marker (green) co-stained with DAPI (blue) for nuclei.
(A) Iba1-positive cells surrounding the cyst. (B) Cell aggregation adjacent to the cyst and it includes many Iba1-positive cells. The asterisk (*) indicates syrinx center. DAPI: 4',6-Diamidino-2-phenylindole; Iba1: ionized calcium-binding adapter molecule 1.

Figure 4 | Comparison between micro-CT and histological measurements.
(A) A comparison between the surface area of syrinxes as measured from micro-CT slices versus histological sections. (B) A comparison based on the cyst volume. In both cases, there was a statistically significant difference between both values. Data is expressed as the mean ± SD; **$P < 0.01$ (paired t-test), $n = 8$ spinal cords. micro-CT: Micro-computed tomography.

3D reconstruction of spinal cords and lesions

The 3D rendering of unfiltered micro-CT data in **Figure 5** shows two spinal cords reconstructed from micro-CT datasets from two different rats. Micro-CT enables researchers to visualize tissues in 3D, and through thresholding and segmentation, lesions can be separated from the surrounding tissue. 3D reconstruction allows for lesion visualization in its near-actual shape as shown in **Figure 5A**. While **Figure 5B** shows the 3D reconstruction of another spinal cord that shows the parenchyma of the spinal containing a large cystic lesion (denoted by arrowheads) and multiple small cysts (indicated by arrows), these 3D figures can be recorded as a video to better visualize the lesion within the spinal cord from multiple perspectives (Additional videos 1 and 2). 3D reconstructing of the shape of the spinal cord would be very difficult to appreciate using histology due to the complicated and lengthy process of 3D reconstruction from histological slides.

Interestingly, **Figure 5** also shows hyperdense lesions on the surface of the spinal cord, likely from Kaolin accumulation. Visualizing the spinal cord and lesions from different
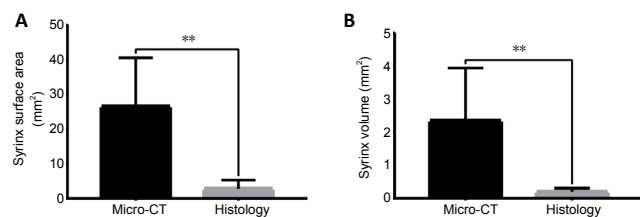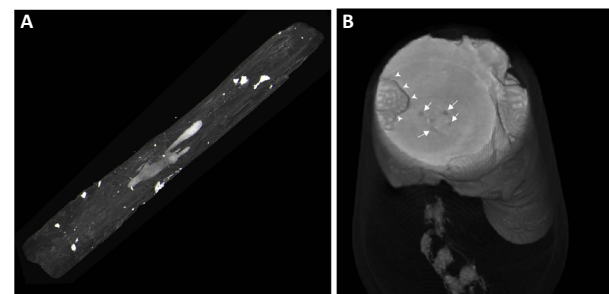

Figure 5 | Three-dimensional reconstruction of micro-computed tomography slices.
it shows a radio-opaque filled intraspinal cyst reconstructed within the spinal cord (A) and spinal cord segmented with a large cyst (B) marked with arrowheads and small defects within the spinal cord parenchyma.

perspectives enable researchers to formulate a 3D relationship between various structure. For instance, with careful inspection of a rotating 3D construct of the spinal cord, it was evident that none of these hyperdense areas seen in **Figure 5** penetrate the spinal cord and their presence is limited to the surface of the spinal cord or its meninges.

Discussion

Few published reports were found on the use of micro-CT for evaluation of cystic lesion within the spinal cord, even though non-invasive techniques, such as micro-CT, provide great appeal to both research and clinical communities due to its non-destructive nature and highly quantitative data that can be generated. For confirmation of syrinx formation and evaluation of syrinx size, currently available techniques mainly include histological techniques and MRI. Histological analysis, even though it is a well-established and widely used method, still has its limitations, especially when it comes to cystic lesions and delicate tissues. Estimating syrinx size using only histological sections may result in inconsistencies due to many reasons. As mentioned earlier, histological analysis limitations include exposing the tissue to distortion due to longitudinal and radial stretching during sectioning (Khimchenko et al., 2016). Previous studies have found that cyst size estimation using traditional histological methods results in an overestimation of the size (Weber et al., 2006) while others found it to be underestimated (Boca et al., 2017), which indicates inconsistencies. Moreover, histological methods are destructive and very difficult to produce accurate 3D information (de Crespigny et al., 2008) due to tissue anisotropy (Chanda and Callaway, 2018). MRI is difficult to substitute for histological analysis or work as an ancillary technique, due to high technical requirements and relatively high costs.

Currently, available micro-CT systems can provide isotropic resolutions at the micron level and 3D rendering with isotropic voxel size (Khimchenko et al., 2016). Importantly micro-CT systems are less expensive and more accessible to researchers compared to MRI. In terms of the goal of determining the viability of micro-CT to evaluate spinal cord lesions, this study found that micro-CT can detect intraparenchymal lesions within the spinal cord with a close match in shape and size to what histology shows. Importantly we showed key advantages over histological analysis such as 3D rendering and the ability to identify specific signal intensity, which allows for more accurate comparisons between different lesions. This close match between the tomographic and histological slices of soft tissues is supported by another study that found similar correspondence between human cerebellum sections evaluated with both techniques (Khimchenko et al., 2016). Visualization of soft tissues using x-ray sometimes is accompanied by artifacts such as bands of different intensity, which may impede detailed description (Müller et al., 2006), such as the distinction between grey matter and white matter in central nervous system tissues. However, these artifacts do not usually impede the detection of cysts due to the vast difference in the signal intensity between a fluid-filled cyst and soft tissues (**Figure 1**). A more recent study (Liao et al., 2017) used a remarkably similar technique to study PTSM. This study used propagation-based synchrotron radiation micro-CT, an imaging technique that gives ultra-high-resolution images of soft tissues compared to conventional micro-CT. The results of the cited study support the claim that micro-CT, either conventionally or through PB-SR, could be a useful tool in assessing the size of spinal cord cysts in experimental animals.

Moreover, new advances in software and reconstruction algorithms make it possible to compensate for such drawbacks (Hsieh et al., 2013; Özkan et al., 2015; Bikis et al., 2018). On the other hand, histological sections sometimes show artifacts such as air bubbles or fractures (Taqi et al., 2018) that may be confused with cell aggregation and cystic lesions. Therefore, this combination of findings provides some support for the conceptual premise that histological analysis of cystic lesions should be performed hand in hand with a non-destructive affordable imaging technique that can overcome some of the common artifacts that inevitably happen during sample preparation, sectioning, mounting, and imaging. The current work highlights the role that micro-CT could play in evaluating neural tissue of rodents in the research setting should it is given due attention.

In the current study, comparing different sections with various materials injected into the spinal cord post-mortem revealed that some of these materials cannot be imaged by micro-CT. The reason can be explained by the fact that they are radio translucent. Another possible explanation is that they have diffused out of the tissue and are no longer present at a detectable level. On the other hand, the ability of micro-CT to detect kaolin as well as a polymer-hydrogel inside the parenchyma of the spinal cord is a valuable finding. For kaolin detection, the importance stems from the fact that it is one of the reagents used to induce the formation of the cyst inside the spinal cord through inducing arachnoiditis. With the help of micro-CT it was found to diffuse from the subarachnoid space into the cyst. Accumulation of kaolin, which is a paste, inside the cyst might cause a mechanical barrier for the cyst to shrink even if the tested treatment is working effectively on the molecular level to decrease the cyst size. Moreover, kaolin can induce further inflammatory reactions. When it comes to the biopolymer, it is crucial to confirm that the drug delivery vehicle is retained within the spinal cord parenchyma. The components of this biopolymer are mixed while injected. It is supposed to gel fast inside the spinal cord parenchyma and to remain in place to work as a drug-releasing vehicle. The injury model used with this biopolymer, the speed of gelation, and the ability of this hydrogel to stay in situ to deliver the quired drugs (Mohrman et al., 2017) are very critical success factors for the success of this drug delivery system. Therefore, these findings have important implications on the injury model used for the study and for developing a drug delivery system that can be maintained within the spinal cord parenchyma for prolonged drug release.

Even though the syrinx size estimation results are contrary to some previous studies that have suggested that histological analysis overestimates lesion size as mentioned before (Weber et al., 2006), many studies found that tissues shrink about 15% after fixation, sectioning, and mounting due to many factors including fixative and intrinsic tissue contractility (Boonstra et al., 1983; Kerns et al., 2008; Tran et al., 2015). Our results showed a much more than 15% reduction in the size of syrinxes were estimated using histology vs. micro-CT. There might be multiple reasons for this. First, these studies measured whole solid organs such as the whole optic nerve, and this makes the histology estimate more accurate than the estimate of cystic lesions that vary in shape in different sections. Moreover, micro-CT shows more precision when it comes to the detection of tiny cysts that can be overlooked by traditional histology. These small lesions that appear in the 3D reconstruction models may not be evident in traditional histological sections, and this may be another explanation for the difference between syrinx size as evaluated using micro-CT and histology. Another possible reason for the evident difference in the estimates is that extrapolation of syrinx size using histology can overlook large cystic areas in the skipped sections. It is possible to collect and image all sections, but this is potentially a laborious effort without some kind of automation, which would take time to optimize and validate on its own. Finally, the quality of histological sections was a challenge at some points, and this may have contributed to errors in estimating syrinx sizes. Even though there are other methods to overcome these challenges, it is not always guaranteed to result in high-quality sections and images.

Limitations

In addition to the previously mentioned limitations, this study did not include a third independent analytical tool such as MRI to verify which of the modalities gave more accurate measurements. The present study adds to the

Research Article

growing body of work indicating the effectiveness of micro-CT imaging in assessing the size of cystic lesions in neural tissues. However, the purpose of this study was not to compare various imaging modalities available for measuring neural tissue lesion size. Additionally, measurement of lesions in histological sections proved to be a labor-intensive process that did not allow as many sections as micro-CT did. Consequently, studies with a greater focus on comparing micro-CT to other imaging modalities with careful validation of data needs to be conducted in the future. In terms of improving histology findings, more spinal cord sections, taken at thinner depths, would improve accuracy. In order to make this feasible, automation or semi-automation needs to be implemented in the sectioning, imaging, and estimating the lesion size. This would make histological results more comparable to micro-CT results.

Conclusions

This study set out to evaluate the utility of micro-CT for investigating cystic lesions in the spinal cord. We used a PTSM rat model to compare micro-CT analysis to conventional histological analysis. The study reveals that micro-CT can detect lesions within the spinal cord very similar to histology. Importantly, micro-CT appears to provide more accurate estimates of the lesions with more measures (e.g., surface area), can detect compounds within the cord, and can be done with the tissue of interest (spinal cord) intact. In summary, both micro-CT and histology are essential for evaluating cystic lesions in the spinal cord, yet histology has limitations. The advantages of using micro-CT imaging for examining these cystic lesions over using traditional histology include shorter processing time after removal of the spinal cord from the animal and the ability to preserve the tissue for any further analysis, including histological analysis. Importantly the suggested approach allows researchers to use both techniques concurrently to increase the productivity of their research and improve the accuracy and reproducibility of lesion size estimation in the spinal cord.

Additional files:
Additional Video 1: Axial reconstruction of a rat spinal cord.
Additional Video 2: Longitudinal reconstruction of a rat spinal cord showing the cystic lesion inside the cord from various perspectives.

References

Al-Shatoury HAH, Galhom AA (2017) Syringomyelia: Background, Pathophysiology, Etiology. Available at: https://emedicine.medscape.com/article/1151685-clinical. Accessed March 1, 2018.

Bikis C, Thalmann P, Degrugillier L, Schulz G, Müller B, Kalbermatten DF, Madduri S, Hieber SE (2018) Three-dimensional and non-destructive characterization of nerves inside conduits using laboratory-based micro computed tomography. J Neurosci Methods 294:59-66.
Boca C, Truyen B, Henin L, Schulte AG, Stachniss V, De Clerck N, Cornelis J, Bottenberg P (2017) Comparison of micro-CT imaging and histology for approximal caries detection. Sci Rep 7:6680.
Boonstra H, Oosterhuis JW, Oosterhuis AM, Fleuren GJ (1983) Cervical tissue shrinkage by formaldehyde fixation, paraffin wax embedding, section cutting and mounting. Virchows Arch A Pathol Anat Histopathol 402:195-201.
Brodbelt AR, Stoodley MA, Watling A, Rogan C, Tu J, Brown CJ, Burke S, Jones NR (2003) The role of excitotoxic injury in post-traumatic syringomyelia. J Neurotrauma 20:883-893.
Campbell GM, Sophocleous A (2014) Quantitative analysis of bone and soft tissue by micro-computed tomography: applications to ex vivo and in vivo studies. Bonekey Rep 3:564.
Chanda A, Callaway C (2018) Tissue anisotropy modeling using soft composite materials. Appl Bionics Biomech 2018:1-9.
Cho KH, Iwasaki Y, Imamura H, Hida K, Abe H (1994) Experimental model of posttraumatic syringomyelia: the role of adhesive arachnoiditis in syrinx formation. J Neurosurg 80:133-139.
Dalkilic T, Fallah N, Noonan VK, Salimi Elizei S, Dong K, Belanger L, Ritchie L, Tsang A, Bourassa-Moreau E, Heran MKS, Paquette SJ, Ailon T, Dea N, Street J, Fisher CG, Dvorak MF, Kwon BK (2018) Predicting injury severity and neurological recovery after acute cervical spinal cord injury: a comparison of cerebrospinal fluid and magnetic resonance imaging biomarkers. J Neurotrauma 35:435-445.
Dauguet J, Delzescaux T, Condé F, Mangin JF, Ayache N, Hantraye P, Frouin V (2007) Three-dimensional reconstruction of stained histological slices and 3D non-linear registration with in-vivo MRI for whole baboon brain. J Neurosci Methods 164:191-204.
de Crespigny A, Bou-Reslan H, Nishimura MC, Phillips H, Carano RAD, D'Arceuil HE (2008) 3D micro-CT imaging of the postmortem brain. J Neurosci Methods 171:207-213.
Disorders NO for R (2016) Heavy Metal Poisoning. Available at: https://rarediseases.org/rare-diseases/syringomyelia/. Accessed October 5, 2019.
Engelhorn T, Eyupoglu IY, Schwarz MA, Karolczak M, Bruenner H, Struffert T, Kalender W, Doerfler A (2009) In vivo micro-CT imaging of rat brain glioma: A comparison with 3 T MRI and histology. Neurosci Lett 458:28-31.
Fraidakis M, Klason T, Cheng H, Olson L, Spenger C (1998) High-resolution MRI of intact and transected rat spinal cord. Exp Neurol 153:299-312.
Gignac PM, Kley NJ (2018) The utility of DiceCT imaging for high-throughput comparative neuroanatomical studies. Brain Behav Evol 91:180-190.
Hemley SJ, Biotech B, Tu J, Stoodley MA (2009) Role of the blood-spinal cord barrier in posttraumatic syringomyelia. J Neurosurg Spine 11:696-704.
Hsieh J, Nett B, Yu Z, Sauer K, Thibault JB, Bouman CA (2013) Recent Advances in CT Image Reconstruction. Curr Radiol Rep 1:39-51.
Kerns MJJ, Darst MA, Olsen TG, Fenster M, Hall P, Grevey S (2008) Shrinkage of cutaneous specimens: formalin or other factors involved? J Cutan Pathol 35:1093-1096.
Khimchenko A, Deyhle H, Schulz G, Schweighauser G, Hench J, Chicherova N, Bikis C, Hieber SE, Müller B (2016) Extending two-dimensional histology into the third dimension through conventional micro computed tomography. Neuroimage 139:26-36.
Klekamp J (2002) The pathophysiology of syringomyelia-historical overview and current concept. Acta Neurochir (Wien) 144:649-664.
Liao S, Ni S, Cao Y, Yin X, Wu T, Lu H, Hu J, Wu H, Lang Y (2017) The 3D characteristics of post-traumatic syringomyelia in a rat model: A propagation-based synchrotron radiation microtomography study. J Synchrotron Radiat 24:1218-1225.
Mohrman AE, Farrag M, Grimm RK, Leipzig ND (2018) Evaluation of in situ gelling chitosan-PEG copolymer for use in the spinal cord. J Biomater Appl 33:435-446.
Mohrman AE, Farrag M, Huang H, Ossowski S, Haft S, Shriver LP, Leipzig ND (2017) Spinal cord transcriptomic and metabolomic analysis after excitotoxic injection injury model of syringomyelia. J Neurotrauma 34:720-733.
Müller B, Riedel M, Thurner PJ (2006) Three-dimensional characterization of cell clusters using synchrotron-radiation-based micro-computed tomography. Microsc Microanal 12:97-105.
Najafi E, Bilston LE, Song X, Bongers A, Stoodley MA, Cheng S, Hemley SJ (2016) Longitudinal measurements of syrinx size in a rat model of posttraumatic syringomyelia. J Neurosurg Spine 24:941-948.
Ohnishi T, Nakamura Y, Tanaka T, Tanaka T, Hashimoto N, Haneishi H, Batchelor TT, Gerstner ER, Taylor JW, Snuderl M, Yagi Y (2016) Deformable image registration between pathological images and MR image via an optical macro image. Pathol Res Pract 212:927-936.
Özkan G, Kanli A, Başeren NM, Arslan U, Tatar İ (2015) Validation of micro-computed tomography for occlusal caries detection: an in vitro study. Braz Oral Res 29:S1806-83242015000100309.
Park HJ, Machado AG, Cooperrider J, Truong-Furmaga H, Johnson M, Krishna V, Chen Z, Gale JT (2013) Semi-automated method for estimating lesion volumes. J Neurosci Methods 213:76-83.
Pixley SK, Hopkins TM, Little KJ, Hom DB (2016) Evaluation of peripheral nerve regeneration through biomaterial conduits via micro-CT imaging. Laryngoscope Investig Otolaryngol 1:185-190.
Saito S, Mori Y, Yoshioka Y, Murase K (2012) High-resolution ex vivo imaging in mouse spinal cord using micro-CT with 11.7T-MRI and myelin staining validation. Neurosci Res 73:337-340.
Schambach SJ, Bag S, Schilling L, Groden C, Brockmann MA (2010) Application of micro-CT in small animal imaging. Methods 50:2-13.
Schwartz ED, Yezierski RP, Pattany PM, Quencer RM, Weaver RG (1999) Diffusion-weighted MR imaging in a rat model of syringomyelia after excitotoxic spinal cord injury. AJNR Am J Neuroradiol 20:1422-1428.
Taqi SA, Sami SA, Sami LB, Zaki SA (2018) A review of artifacts in histopathology. J Oral Maxillofac Pathol 22:279.
Tran T, Sundaram CP, Bahler CD, Eble JN, Grignon DJ, Francesca Monn M, Simper NB, Cheng L (2015) Correcting the shrinkage effects of formalin fixation and tissue processing for renal tumors: Toward standardization of pathological reporting of tumor size. J Cancer 6:759-766.
Webb E, Yuan M, Lemoine N, Wang Y (2016) Imaging in animal models. Integr Cancer Sci Ther 3:428-431.
Weber T, Vroemen M, Behr V, Neuberger T, Jakob P, Haase A, Schuierer G, Bogdahn U, Faber C, Weidner N (2006) In vivo high-resolution MR imaging of neuropathologic changes in the injured rat spinal cord. AJNR Am J Neuroradiol 27:598-604. s
Zehbe R, Haibel A, Riesemeier H, Gross U, Kirkpatrick CJ, Schubert H, Brochhausen C (2010) Going beyond histology. Synchrotron micro-computed tomography as a methodology for biological tissue characterization: from tissue morphology to individual cells. J R Soc Interface 7:49-59.

C-Editors: Zhao M, Li CH; T-Editor: Jia Y